assessment of individual factors so that the more complex interactions between nucleic acids and amino acids can be understood. Clearly, even on the monomer level the interactions between amino acids and nucleotides are sufficiently quantifiable;[8c] if polar interactions are included, a rudimentary "preferential" scheme can be seen: the stability of the adducts decreases within the series $(ATP)(H(trp))^{4-} > (ATP)(H(leu))^{4-} > (ATP)(H(ala))^{4-}$.

In addition, the stability of the ternary $M(ATP)(Aa)^{3-}$ complexes differs not very much for a given metal ion (Table I), but the results of Table V show that the ability to form specific and distinct structures differs; especially the differences for the ternary Zn^{2+} complexes are quite pronounced: in 10^{-3} M solution at pH 7 the "closed" form of $Zn(ATP)(trp)^{3-}$ is favored by a factor of about 30 over the "closed" isomer of $Zn(ATP)(leu)^{3-}$. Hence, these data suggest that evolutionary selectivity in nucleotide/metal ion/amino acid systems is probably not so much achieved, at least for a given metal ion, by differences in complex stability but rather by the ability to form specific and distinct structures.

In summary, via the formation of mixed-ligand complexes certain ligand-ligand associations may be favored and thus distinct structures may be created in a way that involves only small changes from an energetic point of view. Regarding the specificity and selectivity observed in nature, this seems to be the most fascinating point of the present results.

Acknowledgment. We thank Rita Baumbusch for technical assistance, K. Aegerter for recording the 90-MHz ^1H NMR spectra, and the CIBA-Stiftung Basel for support toward the costs of these spectra. The computers were made available by the Rechenzentrum der Universität Basel (UNIVAC 1100/81). These supports and a research grant from the Swiss National Science Foundation are gratefully acknowledged.

Registry No. ATP, 56-65-5; Mn, 7439-96-5; Cu, 7440-50-8; Zn, 7440-66-6; Cd, 7440-43-9; Pb, 7439-92-1; leucine, 61-90-5; norleucine, 327-57-1; norvaline, 6600-40-4; α-aminobutyric acid, 80-60-4; isoleucine, 73-32-5; alanine, 56-41-7; tryptophan, 73-22-3.

Contribution from the Departments of Chemistry, University of Denver, Denver, Colorado 80208, and University of Colorado at Denver, Denver, Colorado 80202

Metal-Nitroxyl Interactions. 27. Comparison of Electron-Electron Spin-Spin Coupling Constants for Urea and Amide Linkages in Spin-Labeled Copper Porphyrins

KUNDALIKA M. MORE, GARETH R. EATON,* and SANDRA S. EATON

Received May 19, 1982

A series of spin-labeled copper porphyrins has been prepared with urea linkages between the porphyrin ring and the nitroxyl ring. The electron-electron coupling constants, J, have been obtained from the solution EPR spectra. The observed values of J are lower by factors of about 2 to >40 for the compounds with urea linkages than for analogous compounds with amide linkages. The decreased values of J for the urea linkages are consistent with a largely σ-bonding pathway for the copper-nitroxyl interaction. In several cases two components were observed in the EPR spectra. These are attributed to different conformations of the porphyrin-nitroxyl linkage.

Introduction

The ability to determine patterns and pathways of electron spin delocalization is important in areas of chemistry ranging from molecular orbital theory and electronic structure to mechanisms of reaction. Recent results from these laboratories have demonstrated that EPR studies of electron-electron spin-spin coupling constants, J, in spin-labeled metal complexes can be used to monitor changes in electron spin delocalization due to changes in coordinated metal,[1,2] changes in metal-nitroxyl linkages,[3-7] and changes in ligand conformation.[4-6] In a study of spin-labeled pyridine adducts of vanadyl and copper(II) bis(hexafluoroacetylacetonates) it was found that the change in J that resulted when an amide linkage between the pyridine and nitroxyl rings was replaced by a urea linkage correlated with the relative importance of σ- and π-delocalization pathways in the metal-nitroxyl interaction.[7] Our previous studies of the values of J for the amide-linked spin-labeled copper porphyrins I-IV indicated that σ-bonding pathways were largely responsible for the electron-electron interaction.[6] We have therefore prepared the analogous urea-linked complexes V-VIII to further explore the interaction pathway in these porphyrins. The spectral data for the amide-linked porphyrins X and XI indicated little π interaction between the porphyrin ring and the amide side chain.[4] Com-

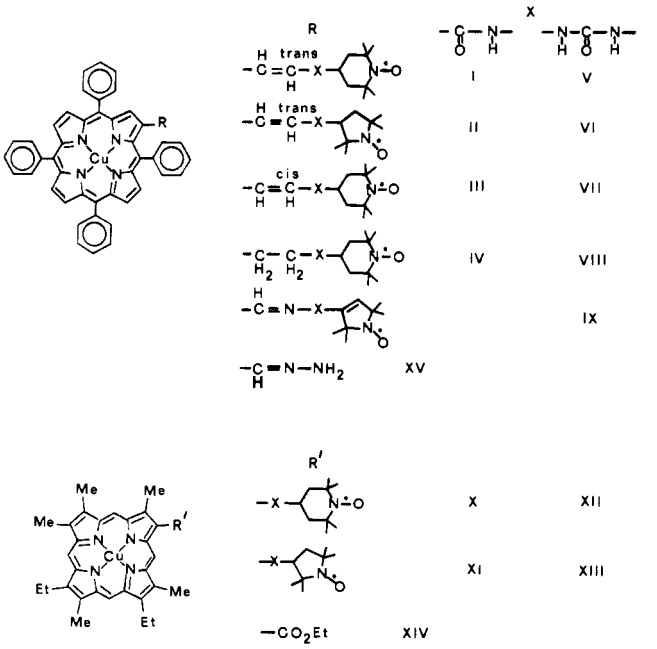

*To whom correspondence should be addressed at the University of Denver.

0020-1669/83/1322-0934$01.50/0

plexes XII and XIII were therefore prepared to give further insight into the importance of π delocalization in these porphyrin derivatives.

Experimental Section

Physical Measurements. Infrared spectra were obtained in halocarbon or Nujol mulls on a Perkin-Elmer 337 or 283B spectrometer. Electronic spectra were obtained in $CHCl_3$ solution on a Beckman Acta V spectrometer. Data are given below with wavelengths in nanometers and log ϵ in parentheses. X-Band EPR spectra were obtained on a Varian E-9 spectrometer. EPR samples were prepared in dried degassed solvents with concentrations about 10^{-3} M. All spectra were obtained at microwave power levels well below saturation. g values were measured relative to that of DPPH (2.0036). Elemental analyses were performed by Spang Microanalytical Laboratory.

Preparation of Compounds. Copper(II) *meso*-Tetraphenyl-2-[2-((((2,2,6,6-tetramethyl-1-oxy-4-piperidinyl)amino)carbonyl)amino)-ethenyl]porphyrin, Trans Isomer (V). Oxalyl chloride (1.26 g, 10 mmol) was added to a solution of copper(II) *meso*-tetraphenylporphyrin-2-*trans*-acrylic acid[8] (0.149 g, 0.2 mmol) in 50 mL of benzene. The mixture was stirred for 2 h at room temperature, taken to dryness under vacuum, and kept under vacuum for 2 h. The residue was dissolved in 200 mL of dry THF/acetone (7:3, v/v). The solution was added dropwise (10 min) to a solution of sodium azide (0.65 g, 10 mmol) in 10 mL of H_2O at 0 °C. After the addition was complete, the solution was stirred for 3 h at 10 °C. The solution was extracted with 50 mL of toluene. The toluene solution was dried over molecular sieves (4A) and then refluxed for 24 h under N_2. The solvent was removed under vacuum. An IR spectrum of the crude isocyanate included a peak at 2240 cm^{-1} characteristic of ν_{NCO}. The solid was dissolved in dry THF (75 mL). 4-Amino-2,2,6,6-tetramethyl-1-oxypiperidine (0.034 g, 0.2 mmol) was added, and the solution was refluxed for 15 h. The solvent was removed under vacuum, and the residue was chromatographed on silica gel in $CHCl_3$ solution. The slow-moving second band contained the product, which was recrystallized from $CHCl_3$/heptane: yield 0.055 g, 30%; IR $\nu_{C=C}$ 1610, $\nu_{C=O}$ 1620, ν_{NH} 3270, 3340 cm^{-1}; Vis 580 (sh, 3.72), 548 (4.14), 421 (5.23). Anal. Calcd for $C_{56}H_{48}CuN_7O_2$: C, 73.54; H, 5.29; N, 10.72. Found: C, 73.34; H, 5.37; N, 10.46.

Copper(II) *meso*-Tetraphenyl-2-[2-((((2,2,5,5-tetramethyl-1-oxy-3-pyrrolidinyl)amino)carbonyl)amino)ethenyl]porphyrin, Trans Isomer (VI). The urea was prepared as reported for V with 3-amino-2,2,5,5-tetramethyl-1-oxypyrrolidine: yield 28%; IR $\nu_{C=C}$ 1610, $\nu_{C=O}$ 1620, ν_{NH} 3270, 3340 cm^{-1}; Vis 580 (sh, 4.00), 548 (4.43), 421 (5.51). Anal. Calcd for $C_{55}H_{46}CuN_7O_2$: C, 73.36; H, 5.15; N, 10.89. Found: C, 73.17; H, 5.29; N, 10.91.

Copper(II) *meso*-Tetraphenyl-2-[2-((((2,2,6,6-tetramethyl-1-oxy-4-piperidinyl)amino)carbonyl)amino)ethenyl]porphyrin, Cis Isomer (VII). The urea was prepared as reported for the trans isomer, V: yield 33%; IR $\nu_{C=C}$ 1610, $\nu_{C=O}$ 1620, ν_{NH} 3350 cm^{-1}; Vis 576 (sh, 3.67), 545 (4.20), 419 (5.36). Anal. Calcd for $C_{56}H_{48}CuN_7O_2$: C, 73.54; H, 5.29; N, 10.72. Found: 73.44; H, 5.17; N, 10.51.

Copper(II) *meso*-Tetraphenyl-2-[2-((((2,2,6,6-tetramethyl-1-oxy-4-piperidinyl)amino)carbonyl)amino)ethyl]porphyrin (VIII). The urea was prepared as reported for the trans isomer V: yield 40%; IR ν_{CO} 1650, ν_{NH} 3360 cm^{-1}; Vis 576 (sh, 3.50), 540 (4.38), 416 (5.76). Anal. Calcd for $C_{56}H_{50}CuN_7O_2$: C, 73.38; H, 5.50; N, 10.70. Found: C, 73.49; H, 5.38; N, 10.75.

Copper(II) *meso*-Tetraphenyl-2-(hydrazonomethyl)porphyrin (XV). Hydrazine (0.064 g, 2 mmol) was added to a solution of copper(II) *meso*-tetraphenyl-2-formylporphyrin[8] (0.703 g, 1 mmol) in toluene (100 mL). The solution was refluxed for 15 h. The solvent was removed under vacuum, and the residue was chromatographed on silica gel in $CHCl_3$ solution. The second dark red band was collected. The product was recrystallized from $CHCl_3$/heptane: yield 0.58 g, 83%; IR $\nu_{C=N}$ 1600, ν_{NH} 3370 cm^{-1}; Vis 580 (sh, 3.63), 546 (4.16), 422 (5.36); EPR ($CHCl_3$) g = 2.0944, A_{Cu} = 86.5 G, A_N = 16.0 G. Anal. Calcd for $C_{45}H_{30}N_6Cu$: C, 75.24; H, 4.21; N, 11.70. Found: C, 75.25; H, 4.18; N, 11.71.

Copper(II) *meso*-Tetraphenyl-2-[2-((((2,2,5,5-tetramethyl-1-oxy-3-pyrrolinyl)amino)carbonyl)hydrazono)methyl]porphyrin (IX). 3-Isocyanato-2,2,5,5-tetramethyl-1-oxypyrroline[9] was added to a solution of copper porphyrin XV (0.143 g, 0.2 mmol) in dry THF (50 mL). The solution was refluxed for 6 h, and then the solvent was removed under vacuum. The product was recrystallized from $CHCl_3$/heptane: yield 0.170 g, 95%; IR $\nu_{C=N}$ 1605, $\nu_{C=O}$ 1620, ν_{NH} 3360 cm^{-1}; Vis 588 (sh, 3.91), 548 (4.20), 428 (5.36). Anal. Calcd for $C_{54}H_{43}CuN_8O_2$: C, 72.10; H, 4.82; N, 12.46. Found: C, 72.16; H, 4.74; N, 12.32.

Copper(II) 2-[(((2,2,6,6-Tetramethyl-1-oxy-4-piperidinyl)amino)-carbonyl)amino]-7,12-diethyl-3,8,13,17,18-pentamethylporphyrin (XII). Thionyl chloride (3 mL) and 2-carboxy-12,17-diethyl-3,7,8,13,18-pentamethylporphyrin[4] (0.096 g, 2 mmol) in dry THF/acetone (7:3 v/v, 100 mL) were added dropwise, over a 10-min interval, to a solution of sodium azide (0.65 g, 10 mmol) in 10 mL of H_2O at 0 °C in the absence of light. The mixture was stirred for 3 h at 10 °C. The product was extracted into cold toluene, and the toluene solution was dried over molecular sieves (4A) in the refrigerator overnight. The toluene solution was then stirred at 60 °C for 4 h. After removal of the solvent under vacuum the crude product had a characteristic ν_{NCO} at 2240 cm^{-1}. The solid was dissolved in THF (75 mL), and 4-amino-2,2,6,6-tetramethyl-1-oxypiperidine (0.034 g, 0.2 mmol) was added. After the solution was stirred for 6 h at 50 °C, the solvent was removed under vacuum. The residue was chromatographed on silica gel in $CHCl_3$ solution. The first band was collected and reduced in volume to 30 mL. Copper acetate (0.04 g, 0.2 mmol) in 2 mL of boiling methanol was added, and the solution was refluxed for 10 min. The solvent was removed under vacuum, and the residue was chromatographed on silica gel in $CHCl_3$. The second slow-moving red band contained the product, which was then recrystallized from CH_2Cl_2/hexane: yield 0.028 g, 20%; IR ν_{CO} 1630, ν_{NH} 3270, 3340 cm^{-1}; Vis 570 (4.28), 533 (4.23), 406 (5.50). Anal. Calcd for $C_{39}H_{48}CuN_7O_2 \cdot 0.43CH_2Cl_2$: C, 63.41; H, 6.59; N, 13.13; Cl 4.07. Found: C, 63.24; H, 6.33; N, 13.34; Cl, 3.76. We have also observed in studies of related compounds that chlorinated solvents are held strongly in the crystal lattice.[4]

Copper(II) 2-[((((2,2,5,5-Tetramethyl-1-oxy-3-pyrrolidinyl)-amino)carbonyl)amino]-7,12-diethyl-3,8,13,17,18-pentamethylporphyrin (XIII). The urea was prepared as reported for XII with 3-amino-2,2,5,5-tetramethyl-1-oxypyrrolidine. Recrystallization was from $CHCl_3$/heptane: yield 20%; IR ν_{CO} 1640, ν_{NH} 3270, 3340 cm^{-1}; Vis 568 (4.26), 537 (4.25), 410 (5.41). Anal. Calcd for $C_{38}H_{46}CuN_7O_2 \cdot 0.34CHCl_3$: C, 62.49; H, 6.34; N, 13.30; Cl, 4.91. Found: C, 62.25; H, 6.12; N, 13.43; Cl, 4.66.

Computer Simulations. For a molecule containing two unpaired electrons and no nuclear spins the EPR Hamiltonian for fluid solution spectra is given by eq 1. It is assumed that molecular tumbling is

$$H = \beta\vec{H}(g_1\vec{S}_1 + g_2\vec{S}_2) + hJ\vec{S}_1\cdot\vec{S}_2 \quad (1)$$

sufficiently rapid to fully average anisotropic interactions. The computer program CUNO[2,10] was used to obtain the computer simulations reported here. It uses eq 1 plus terms arising from nuclear hyperfine coupling to the copper nucleus (A_{Cu}), to nitrogens in the copper coordination sphere (A_N), and to the nitroxyl nitrogen ($A_{N'}$). The sign of J cannot be determined from these experiments. Detailed discussions of the calculations have been provided.[2,10]

To facilitate comparison with the field-swept experimental spectra, the values of J, A_M, A_N, and $A_{N'}$ are in units of gauss. The conversion

(1) More, K. M.; Eaton, S. S.; Eaton, G. R. *J. Am. Chem. Soc.* **1981**, *103*, 1087–1090.
(2) Sawant, B. M.; Shroyer, A. L. W.; Eaton, G. R.; Eaton, S. S. *Inorg. Chem.* **1982**, *21*, 1093–1101.
(3) More, K. M.; Eaton, S. S.; Eaton, G. R. *Inorg. Chem.* **1981**, *20*, 2641–2647.
(4) Sawant, B. M.; Braden, G. A.; Smith, R. E.; Eaton, G. R.; Eaton, S. S. *Inorg. Chem.* **1981**, *20*, 3349–3354.
(5) More, K. M.; Sawant, B. M.; Eaton, G. R.; Eaton, S. S. *Inorg. Chem.* **1981**, *20*, 3356–3362.
(6) More, K. M.; Eaton, G. R.; Eaton, S. S. *Can. J. Chem.* **1982**, *60*, 1392–1401.
(7) More, J. K.; More, K. M.; Eaton, G. R.; Eaton, S. S. *Inorg. Chem.* **1982**, *21*, 2455–2460.
(8) Momenteau, M.; Loock, B.; Bisagni, E.; Rougee, M. *Can. J. Chem.* **1979**, *57*, 1804–1813 (in this paper and in our previous papers on related compounds, the carbon to which the acrylic acid group was attached was denoted the 1-carbon).
(9) DuBois, D. L.; Eaton, G. R.; Eaton, S. S. *J. Am. Chem. Soc.* **1978**, *100*, 2686–2689.
(10) Eaton, S. S.; DuBois, D. L.; Eaton, G. R. *J. Magn. Reson.* **1978**, *32*, 251–263.

between hertz and gauss is given by eq 2–4. g_1 and g_2 are the copper

$$J\,(\mathrm{G}) = [J\,(\mathrm{Hz})]\frac{h}{2\beta}\left(\frac{1}{g_1}+\frac{1}{g_2}\right) \quad (2)$$

$$A_{\mathrm{M}}\,(\mathrm{G}) = [A_{\mathrm{M}}\,(\mathrm{Hz})]\frac{h}{g_1\beta} \quad (3)$$

$$A_{\mathrm{N}'}\,(\mathrm{G}) = [A_{\mathrm{N}'}\,(\mathrm{Hz})]\frac{h}{g_2\beta} \quad (4)$$

and nitroxyl g values, respectively. The conversion factor for A_{N} is the same as for A_{M}.

The electron–electron spin–spin coupling results in AB patterns in the EPR spectra. The lines in the spectra are referred to as copper or nitroxyl depending on the nature of the transition as $J \rightarrow 0$. When J is small relative to the g-value difference between the copper and nitroxyl electrons, each of the copper and nitroxyl lines is split into a doublet. In the spin-labeled copper porphyrins reported here, the copper line widths are much greater than the nitroxyl line widths so the splittings due to small values of J are resolved for the nitroxyl lines but not for the copper lines. As J becomes larger, the intensities of the outer lines of the AB patterns go to zero and the positions of the inner copper and inner nitroxyl lines become equal.

The EPR parameters for XIV and CuTPP (g = 2.0944, A_{Cu} = 86.5 G, and A_{N} = 16.0 G in $CHCl_3$ solution and g = 2.0994, A_{Cu} = 82.0 G, and A_{N} = 15.5 G in pyridine solution) were used as starting parameters in simulating the EPR spectra of the spin-labeled complexes. In all cases the best fits to the spectra of the spin-labeled complexes were obtained with values for g_1, A_{Cu}, and A_{N} that fell within the range observed for XIV and CuTPP in $CHCl_3$ and pyridine solutions. The nitroxyl parameters were g = 2.0059 ± 0.0001 and A_{N} = 14.8–16.8 G depending on solvent, temperature, and ring size. The values of J obtained from the simulations are given in Tables I and II. The values of the parameters used to obtain the simulations shown in Figures 1 and 2 are given in Table III. These values are typical of the ones used in all the simulations.

Results and Discussion

The urea linkages in these spin-labeled porphyrins were prepared by the conversion of acid chlorides to isocyanates and condensation of the isocyanates with amines. The urea linkages are stable to chromatography on silica gel and require no special handling. The complexes have been characterized by IR and visible spectroscopy and elemental analyses.

Tetraphenylporphyrin Derivatives. Spin-labeled copper porphyrin V has trans olefin and urea linkages between the pyrrole carbon and a piperidine nitroxyl ring. The EPR spectra of the nitroxyl lines in $CHCl_3$ or pyridine solution are a doublet of triplets with J = 6.5 or 5.7 G, respectively, at room temperature. These values of J are less than the copper line widths so no splitting is observed for the copper lines. In the analogous compound I containing an amide linkage in place of the urea linkage, J at room temperature was found to be 19.9 G in $CHCl_3$ solution and 25.6 G in pyridine solution.[6] Thus, the change from an amide linkage to a urea linkage reduces the value of J by a factor of 3–5, depending on the solvent. For both I and V the value of J increases with decreasing temperature (Table II) but the difference between the two linkages at −60 °C is similar to that at room temperature.

Complexes II and VI provide a similar comparison, but this case involves a five-membered pyrrolidine ring. The values of J are smaller for the urea than for the amide with decreases ranging from a factor of about 2.5 to >5, depending on solvent and temperature. We have previously observed that values of J for compounds containing the pyrrolidine nitroxyl are more solvent and temperature dependent than for other nitroxyls.[4,6]

When the olefin is cis instead of trans as in urea VII, no splitting is observed in the nitroxyl signals in a variety of solvents at room temperature or in CH_2Cl_2 solution at −80 °C.

Table I. Electron–Electron Coupling Constants, J, at Room Temperature[a]

compd	solvent	X: -N(H)-C(=O)-	X: -N(H)-C(=O)-N(H)-
		I	V
CuTPP–C(H)=C(H)–X–N•–O (trans)	$CHCl_3$	19.9[b]	6.5
	pyridine	25.6[b]	5.7
		II	VI
CuTPP–C(H)=C(H)–X–N•–O (trans)	$CHCl_3$	3[b]	<1
	pyridine	5.2[b]	<1
		III	VII
CuTPP–C(H)=C(H)–X–N•–O (cis)	$CHCl_3$	<1[b]	<1
	pyridine	3.5[b]	<1
		IV	VIII
CuTPP–CH_2–CH_2–X–N•–O	$CHCl_3$	9.3[b]	<1
	pyridine	13.5[b]	<1.5
			IX
CuTPP–C(H)=N–X–N•–O	$CHCl_3$		13
	toluene		23.5
	THF		26.0
	pyridine		37.0
		X	XII
CuP–X–N•–O	$CHCl_3$	78[c]	<2
	CH_2Cl_2	82[c]	<2
	pyridine	90[c]	4.3, 38.5 (1:1)[d]
		XI	XIII
CuP–X–N•–O	CH_2Cl_2	~100[c]	9, 36 (3:2)[d]
	pyridine	~100[c]	23, 80 (1:2)[d]

[a] Values are given in gauss for spectra taken at X band at 22–27 °C. [b] Value taken from ref 6. [c] Value taken from ref 4. [d] Two components are observed in the spectra. The ratio of the populations is given in parentheses.

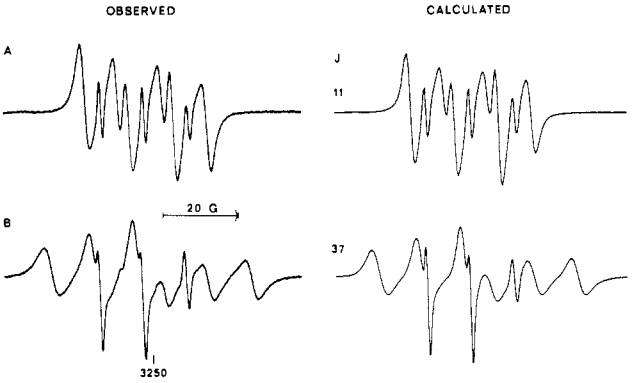

Figure 1. X-band (9.11-GHz) EPR of the nitroxyl region of the spectra of spin-labeled copper porphyrin IX at room temperature and computer simulations: (A) CH_2Cl_2 solution, 100-G scan obtained with 0.5-G modulation amplitude and 2-mW power; (B) pyridine solution, 100-G scan obtained with 0.8-G modulation amplitude and 0.5-mW power. Values of J are in gauss.

Since the value of J for the analogous amide III is 6.0 G at −80 °C, the urea linkage in this isomer reduces the value of J by more than a factor of 6.

When the olefin is converted to a saturated linkage as in VIII, no splitting is observed in the nitroxyl signals at room temperature, but at −80 °C, J = 3.5 G in CH_2Cl_2 solution. Comparison with the amide analogue IV shows that the urea linkage reduces the value of J by a factor of 6 to >10. Thus the impact of the urea linkage is substantial for each of the pairs but is greater for the cis olefin and the saturated ethane linkage than for the trans olefin. In a study of spin-labeled pyridine adducts of vanadyl and copper(II) bis(β-diketonates)

Table II. Temperature Dependence of Electron–Electron Coupling Constants[a]

compd	X: -N(H)-C(=O)-b	X: -N(H)-C(=O)-N(H)-c
CuTPP—C(H)=C(H)—X—(N—O) trans	I 25.6 (22)[d] 3.2 (−60)[d]	V 5.0 (27) 9.0 (−60)
CuTPP—C(H)=C(H)—X—(N•—O) trans	II 5 (22)[d] 5 (−60)[d]	VI <1 (27) 2.2 (−80)
CuTPP—C(H)=C(H)—X—(N•—O) cis	III 3.5 (22)[d] 6.0 (−60)[d]	VII <1 (27) <1 (−80)
CuTPP—CH_2CH_2—X—(N—O)	IV 14.0 (22)[d] 3, 22 (1:2) (−60)[d]	VIII <1 (27) 3.5 (−80)
CuTPP—C(H)=N—X—(N•—O)		IX 11 8 (−61)
CuP—X—(N•—O)		XII[e] 4, 38 (2:1) (27) 8, 44 (2:1) (−50)

[a] Values are given in gauss for spectra taken at X band; temperatures (in °C) are given in parentheses. [b] Spectra taken in 2:1 toluene–pyridine solution. [c] Spectra taken in CH_2Cl_2 solution unless otherwise noted. [d] Values taken from ref 6. [e] Spectra taken in THF solution.

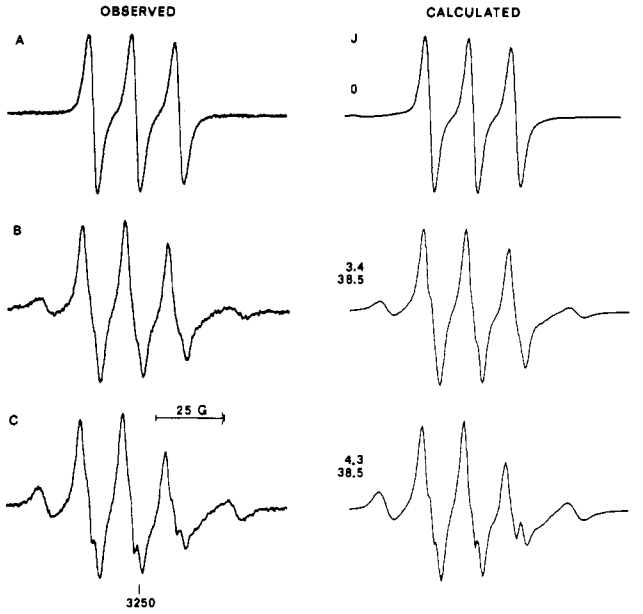

Figure 2. X-band (9.11-GHz) EPR of the nitroxyl region of the spectra of spin-labeled copper porphyrin XII at room temperature and computer simulations: (A) $CHCl_3$ solution, 100-G scan obtained with 0.5 G modulation amplitude and 1-mW power; (B) 1:1 $CHCl_3$–pyridine solution, 100-G scan obtained with 0.5-G modulation amplitude and 2-mW power (there is a 2:1 ratio of populations of the components with J = 3.4 and 38.5 G); (C) pyridine solution, 100-G scan obtained with 0.63-G modulation amplitude and 1-mW power (there is a 1:1 ratio of populations of the two components).

it was observed that the relative magnitude of J for amide and urea linkages was strongly dependent on the mechanism of spin delocalization.[7] Similar values of J were observed for amide and urea linkages when π-delocalization pathways made a substantial contribution to the metal–nitroxyl interaction. In one pair of compounds in which there was a large π contribution to the electron delocalization, the value of J was larger for the urea than for the amide.[7] When σ delocalization dominated the metal–nitroxyl interaction, the change from an amide to a urea linkage caused J to decrease by a factor of 10–100.[7] On this basis it appears that there is a small π contribution to the spin–spin interaction for the trans olefin and a negligible π contribution for the cis olefin and saturated linkages. These results are consistent with our previous conclusion that σ interaction dominated for these systems.[6] It is

Table III. Parameters Used in Simulations of EPR Spectra[a]

figure	component	J, G	g_M	g_{NO}	A_M, G	A_{NO}, G		line width parameters[b] A	B	C
1A	IX	11	2.0944	2.0059	86.5	14.8	Cu	26.7	22.4	6.0
							NO(i)	2.6	0.10	0.0
							NO(o)	3.0	−0.10	0.0
	nitroxyl (3%)[c]			2.0059		14.8		1.5	−0.10	0.10
1B	IX	37.0	2.0994	2.0057	82.0	14.8	Cu	28.7	22.4	5.9
							NO(i)	3.8	0.75	0.25
							NO(o)	4.5	0.0	0.0
	nitroxyl (2%)[c]			2.0060		14.6		1.2	−0.25	0.25
2A	XII	0.0	2.0944	2.0059	86.5	15.8	Cu	26.7	22.4	6.0
							NO	3.5	−0.10	0.10
2B	XIIa (67%)	3.4	2.0972	2.0059	84.0	15.7	Cu	28.7	22.4	5.9
							NO(i)	3.0	−0.05	0.15
							NO(o)	3.1	−0.15	0.15
	XIIb (33%)	38.5	2.0972	2.0057	84.0	15.5	Cu	28.7	22.4	5.9
							NO(i)	5.0	0.0	0.0
							NO(o)	5.3	0.0	0.0
	nitroxyl (2%)[c]			2.0059		15.5		1.5	−0.15	0.15
2C	XIIa (50%)	4.3	2.0994	2.0059	82.0	15.5	Cu	35.0	22.4	5.9
							NO(i)	2.8	−0.10	0.30
							NO(o)	3.0	−0.40	0.40
	XIIb (50%)	38.5	2.0994	2.0057	82.0	15.5	Cu	35.0	22.4	5.9
							NO(i)	5.0	0.0	0.0
							NO(o)	5.5	0.0	0.0
	nitroxyl (2%)[c]			2.0059		15.6		1.7	−0.20	0.20

[a] Percentages are based on the total concentration of the spin-labeled copper complex. [b] A, B, and C are the coefficients in the equation line width = $A + BM_I + CM_I^2$, where M_I is the copper nuclear spin or the nitroxyl nitrogen nuclear spin. Inner and outer lines of the AB patterns are denoted by (i) and (o), respectively. Values for the copper lines are quite uncertain due to incomplete motional averaging. [c] Nitroxyl impurity that is not interacting with a copper electron spin.

also consistent with ENDOR results that indicate primarily σ-spin delocalization to the pyrrole protons of CuTPP.[11]

Complex IX contains a Schiff base linkage in place of the olefinic linkages in V–VII. The values of J for IX are strongly solvent dependent, ranging from 11.0 G in CH_2Cl_2 to 37 G in pyridine solution (Figure 1). In mixtures of CH_2Cl_2 and pyridine a single species is observed but the value of J varies continuously with solvent composition. Values of J in other solvents are given in Table I. These results suggest that two or more conformations of the molecule with significantly different values of J are in rapid equilibrium on the EPR time scale and that the equilibrium is strongly solvent dependent. Several possible equilibria are discussed below. The observation that J is larger for IX in the coordinating solvents THF and pyridine than in the noncoordinating solvents toluene and CH_2Cl_2 suggests the possibility that coordination of a fifth ligand to the copper porphyrin may lead to an increase in the value of J. The equilibrium constant for coordination of pyridine to CuTPP is about 1, and the rate of ligand exchange is fast on the EPR time scale.[5] At the low copper porphyrin concentrations used in these EPR studies, the small binding constant requires that pure pyridine be used as the solvent to effect complete conversion to the pyridine adduct. Under these conditions it is difficult to unambiguously separate the impact of pyridine coordination from the general solvation effects of pyridine. For the other spin-labeled copper porphyrins reported here and for closely related compounds[3,4] a small increase in J is often observed on going from noncoordinating to coordinating solvents. Although pyridine coordination may cause some change in J, it seems unlikely that the large solvent dependence for IX is due predominantly to the presence or absence of a coordinating ligand on the copper. In another spin-labeled copper porphyrin it was observed that the interaction of chlorinated solvents with the nitroxyl moiety or with a group in the vicinity of the nitroxyl resulted in a decrease in the value of J and an increase in the barrier to conformational change.[3,6] For IX the low value of J in $CHCl_3$ and CH_2Cl_2 solution may be due to a similar interaction. Interaction at the nitroxyl could cause a change in spin density and a resultant decrease in J. Interaction with the urea linkage could cause a conformational change that would decrease the value of J. This, however, would not explain the smaller value of J in toluene than in pyridine. Other solvent effects on the urea–nitroxyl linkage also appear to be involved.

Alkylporphyrin Derivatives. The EPR spectra of the spin-labeled porphyrin XII are strongly dependent on solvent as shown in Figure 2. In CH_2Cl_2 or $CHCl_3$ solution (Figure 2A) the nitroxyl region of the spectrum is a triplet with line widths of about 3.5 G. On the basis of computer simulations a value of $J \geq 2$ G would result in an observable change in the line shape at these line widths. Thus, the value of J in these solvents is <2 G. In a 1:1 $CHCl_3$–pyridine mixture (Figure 2B) two components are observed in the EPR spectra with J = 3.4 and 38.5 G and a 2:1 ratio of populations. In pyridine (Figure 2C) the values of J are 4.3 and 38.5 G and the two forms are equally populated. The spectra in THF solution are similar to those in 1:1 CH_2Cl_2–pyridine. When the THF solution was cooled to −60 °C, the values of J increased slightly and the populations of the two species remained approximately at 2:1. For the analogous amide X the values of J in similar solvents are 78–90 G. Thus, the values of J for the two forms of XII are reduced by factors of about 2 and 40, respectively, from those observed for X.

Complex XIII contains a pyrrolidine nitroxyl in place of the piperidine nitroxyl in XII. For XII in $CHCl_3$ solution two species are observed with a 3:2 ratio of populations and values of J of 9 and 36 G, respectively. In pyridine solution the values of J increase to 23 and 80 G and the population ratio changes to 1:2. The values of J are again smaller than for the analogous amide XI, but the strong temperature dependence of the values of J for XI makes a quantitative estimate of the differences imprudent.[4]

Comparison of the data for ureas XII and XIII indicates that for both complexes there are two forms with substantial differences in the values of J, that the population of the species with the larger value of J is greater in pyridine solution than in CH_2Cl_2 solution, and that the values of J are larger in pyridine solution than in CH_2Cl_2 solution. If these changes were due to coordination of pyridine to copper, similar populations of the two forms might be expected for XII and XIII. The large difference in populations of the two forms of XII and XIII in CH_2Cl_2 solution argues against this interpretation. It seems more likely that the conformations of the urea–nitroxyl linkage are strongly solvent dependent. Donor–acceptor interactions between the nitroxyl and the halogenated solvent as discussed above may also contribute to the small values of J in $CHCl_3$ and CH_2Cl_2 solution.

The substantial effects of both solvent and temperature on ligand conformations introduces considerable ambiguity into the discussion of the impact on J of an additional atom in the metal–nitroxyl linkage. There is little information in the literature to permit distinctions to be made between specific solvent interactions and general solvent effects so the selection of optimum solvents for comparison is not straightforward. The choice of solvents in these studies was determined by the limited solubilities of the compounds.

Interaction through σ systems is conformation dependent due to the details of orbital overlaps. For example, "W-plan" conformations have been demonstrated to enhance spin–spin interactions.[12] This was concluded to be the reason that J was larger for I and IV than for III[6] and larger for V than for VII. Part of the solvent dependence of J may reflect the influence of solvation on relative stabilities of W-plan conformations. In nitroxyl diradicals the values of J in σ-bonded systems have also been observed to be strongly dependent on conformation.[13]

Conclusions. Six pairs of spin-labeled copper porphyrins have been examined in which the spin label is attached by a urea or amide linkage to a pyrrole carbon of the porphyrin or to a group attached to the pyrrole carbon. In each case the value of J is smaller by a factor of 2 to >40 for the urea linkage than for the amide linkage. The large decrease in the value of J parallels results for other systems where the electron–electron spin–spin interaction occurred largely through σ-bonding pathways.[7] These interactions are occurring over distances of about 12–16 Å.

For three of the compounds the EPR spectra indicated that the urea–nitroxyl linkage could adopt two or more conformations, which resulted in different values of J. In two cases (XII and XIII) interconversion of the conformations was slow on the EPR time scale and for the third (IX) it was fast on the EPR time scale. We previously obtained evidence for several conformations in another spin-labeled copper porphyrin containing a urea linkage.[5] Thus, there appear to be a greater variety of conformations accessible to urea linkages than to amide linkages.

Acknowledgment. This work was supported in part by NIH Grant GM21156.

Registry No. V, 84433-34-1; VI, 84433-35-2; VII, 84518-21-8; VIII, 84433-36-3; IX, 84433-37-4; XII, 84433-38-5; XIII, 84433-39-6;

(11) Brown, T. G.; Hoffman, B. M. *Mol. Phys.* **1980**, *39*, 1073–1109.

(12) King, F. W. *Chem. Rev.* **1976**, *76*, 157–186.

(13) Parmon, V. N.; Kokorin, A. I.; Zhidomirov, G. M. *Zh. Strukt. Khim.* **1977**, *18*, 132–177; *J. Struct. Chem.* (*Engl. Transl.*) **1977**, *18*, 104–147.

XV, 84433-40-9; *meso*-tetraphenylporphyrin-2-*trans*-acrylic acid, 77698-95-4; 4-amino-2,2,6,6-tetramethyl-1-oxypiperidine, 14691-88-4; 3-amino-2,2,5,5-tetramethyl-1-oxy-pyrrolidine, 34272-83-8; *meso*-tetraphenylporphyrin-2-*cis*-acrylic acid, 77629-57-3; *meso*-tetraphenylporphyrin-2-propanoic acid, 83037-22-3; copper(II) *meso*-tetraphenyl-2-formylporphyrin, 71763-49-0; 3-isocyanato-2,2,5,5-tetramethyl-1-oxypyrroline, 68212-42-0; 2-carboxy-12,17-diethyl-3,7,8,13,18-pentamethylporphyrin, 43012-54-0.

Contribution from the Department of Chemistry,
Harvard University, Cambridge, Massachusetts 02138

The Homogeneous Hydrogen-Evolving Systems $[Mo_2Fe_6S_8(SPh)_9]^{4-,5-}/C_6H_5SH$: Reaction Characteristics, Kinetics, and Possible Mechanisms

T. YAMAMURA,[1a] G. CHRISTOU,[1b] and R. H. HOLM*

Received August 3, 1982

The reduced clusters $[Mo_2Fe_6S_8(SPh)_9]^{4-,5-}$ ([4-], [5-]) and $[Fe_4S_4(SPh)_4]^{3-}$ evolve H_2 from benzenethiol in solutions of purified *N,N'*-dimethylacetamide at ambient temperature. With 500 equiv of thiol clusters [4-] and [5-] afford 86% and ~100% H_2 yields, respectively, after 24 h. Cluster [5-] also produces H_2 from a variety of other protic sources including an 83% yield from 2 equiv of Et_3NH^+ after 24 h. Both [5-]/PhSH and [4-]/PhSH systems generate a common intermediate (Im), which is the last kinetically resolvable species prior to H_2 evolution, experimentally expressible as $d[H_2]/dt = K[Im][PhSH]$. Analysis of H_2 evolution rates in the [4-]/PhSH system leads to the experimental rate law $d[H_2]/dt = [4-]^2[PhSH]^2/\{2300([3-] + 0.00043)[PhS^-] + 0.014[PhSH]\}$. The kinetics of a large number of reaction schemes were theoretically analyzed. Acceptable schemes are those that conform to the preceding rate laws and other experimental constraints. From these the simplest chemically reasonable schemes are proposed for Im formation in the [5-]/PhSH system and H_2 evolution in the [4-]/PhSH system. The latter is considered to be

$$[4-] \underset{RS^-}{\overset{RSH}{\rightleftharpoons}} [4-]\cdot H^+ \underset{[3-]}{\overset{[4-]}{\rightleftharpoons}} [5-]\cdot H^+ \rightleftharpoons Im \rightarrow H_2$$

involving cluster protonation, electron transfer, Im formation, and H_2 evolution. The reaction sequence is presumably driven by the demonstrated irreversibility of the overall reaction $2[4-] + 2PhSH \rightarrow 2[3-] + 2PhS^- + H_2$. Details of the kinetic analysis and alternative schemes are presented. The potential advantage of a two-electron carrier for reduction of H^+ (to hydride) and other two-electron substrates is noted. In this work this advantage is expressed in the proposed and alternative reaction schemes and is experimentally demonstrated by a 42% H_2 yield from the one-electron reductant $[Fe_4S_4(SPh)_4]^{3-}$ and ~500 equiv of PhSH after 24 h.

Introduction

Hydrogenases are uni- or bidirectional catalysts of reaction 1 in the presence of a suitable electron carrier $C_{ox,red}$. This and subsequent reactions are collected in Table I. Characterization of these enzymes,[2,3] which contain Fe-S cluster(s)[4] that presumably function as internal electron-transfer sites and/or the catalytic center itself, is clearly in an accelerating phase. While the enzyme kinetics of several hydrogenases have been elucidated, little is known of reaction mechanisms at a molecular basis other than the intervention of enzyme-hydride intermediates.[3] Consequently, kinetic and mechanistic investigations of stoichiometric and catalytic $2H^+/H_2$ processes effected by well-defined metal species could provide information pertinent to an eventually satisfactory description of enzyme action.

Activation of dihydrogen by the uptake reaction eq 2, involving heterolytic cleavage to form a metal hydride and often facilitated by a general base B, is a well-developed subject.[5-7] The formation of HD in the reverse reaction of systems containing D_2 and a protic solvent with complexes of, e.g., Ag(I), Cu(II), and Ru(III),[5,7-9] constitutes strong evidence for hydride formation. In contrast, spontaneous dihydrogen evolution from a protic source HA by a reducing metal complex or cluster (not introduced as a preformed hydride) in homogenous solutions has received substantially less attention. Synthetic, homogeneous, dihydrogen-evolving systems of this sort have been described,[10-15] several of which are based on unidentified Fe-S-SR species,[11,14] but kinetic and mechanistic details are lacking. Dihydrogen formation by reactions 3, in which M is a mono- or polynuclear species capable of two-electron transfer to substrate, is likely in these cases. In the $Ru(bpy)_3^0/CH_3CN/D_2O$ system the detection of D_2, and no HD from H atom abstraction from acetonitrile by D·, is consistent with a hydride intermediate.[13] Further evidence for such

(1) (a) On leave from Department of Chemistry, Faculty of Science, University of Tokyo. (b) U.K. Science Research Council/NATO Postdoctoral Fellow, 1980-1981.
(2) Schlegel, H. G.; Schneider, K., Eds. "Hydrogenases: Their Catalytic Activity, Structure, and Function"; Erich Goltze KG: Göttingen, 1978.
(3) Adams, M. W. W.; Mortenson, L. E.; Chen, J.-S. *Biochim. Biophys. Acta* **1981**, *594*, 105.
(4) Several hydrogenases recently have been found to contain nickel: Albracht, S. P. J.; Graf, E.-G.; Thauer, R. K. *FEBS Lett.* **1982**, *140*, 311. LeGall, J.; Ljungdahl, P. O.; Moura, I.; Peck, H. D., Jr.; Xavier, A. V.; Moura, J. J. G.; Teixera, M.; Huynh, B. H.; DerVartanian, D. V. *Biochem. Biophys. Res. Commun.* **1982**, *106*, 610.
(5) James, B. R. "Homogeneous Hydrogenation"; Wiley: New York, 1973.
(6) James, B. R. *Adv. Organomet. Chem.* **1979**, *17*, 319.
(7) Brothers, P. J. *Prog. Inorg. Chem.* **1981**, *28*, 1.
(8) (a) Webster, A. H.; Halpern, J. *J. Phys. Chem.* **1957**, *61*, 1239. (b) Schindewolf, U. *Ber. Bunsenges. Phys. Chem.* **1963**, *67*, 219. (c) von Hahn, H. E. A.; Peters, E. *J. Phys. Chem.* **1971**, *75*, 571.
(9) Harrod, J. F.; Cicconi, S.; Halpern, J. *Can. J. Chem.* **1966**, *39*, 1372.
(10) Christensen, R. J.; Espenson, J. H.; Butcher, A. B. *Inorg. Chem.* **1973**, *12*, 564.
(11) Tano, K.; Schrauzer, G. N. *J. Am. Chem. Soc.* **1975**, *97*, 5404.
(12) Nikonova, L. A.; Isaeva, S. A.; Pershikova, N. I.; Shilov, A. E. *J. Mol. Catal.* **1975/1976**, *1*, 367.
(13) Abruña, H. D.; Teng, A. Y.; Samuels, G. J.; Meyer, T. J. *J. Am. Chem. Soc.* **1979**, *101*, 6746.
(14) Okura, I.; Nakamura, S.; Nakamura, K.-I. *J. Mol. Catal.* **1979**, *6*, 71. Okura, I.; Nakamura, S. *Ibid.* **1980**, *9*, 125. Okura, I.; Nakamura, S.; Kobayashi, M. *Bull. Chem. Soc. Jpn.* **1981**, *54*, 3794.
(15) Schrauzer, G. N.; Palmer, M. R. *J. Am. Chem. Soc.* **1981**, *103*, 2659.

0020-1669/83/1322-0939$01.50/0